Enhancing Moon Crescent Visibility Using Contrast-Limited Adaptive Histogram Equalization and Bilateral Filtering Techniques

Wan Nural Jawahir Hj Wan Yussof[1], Mustafa Man[1], Roslan Umar[2], Ahmad Najmuddin Zulkeflee[2], Ezmahamrul Afreen Awalludin[1], and Nazhatulshima Ahmad[3]

[1] *Universiti Malaysia Terengganu, Malaysia,* [2] *Universiti Sultan Zainal Abidin, Malaysia,* [3] *University of Malaya, Malaysia*

Abstract—Image enhancement is becoming increasingly important with the advancement of space exploration techniques and the technological development of more durable and scientifically sound observatories equipped with more powerful telescopes. The enhancement of images helps astronomers analyze the results and act toward determining the dates of religious festivals. This work describes a technique known as contrast-limited adaptive histogram equalization (CLAHE) with grayscale contrast enhancement and bilateral filtering. We apply CLAHE on the L component of the CIE-Lab color space to adjust lightness contrast. Subsequently, grayscale contrast enhancement is performed to increase the visibility of the moon crescent. Noise caused by grayscale contrast enhancement is reduced using bilateral filtering. Two quantitative measures are selected (PSNR and MSE) to show the visual improvement achieved by the proposed algorithm.

Keywords— bilateral filtering, CIE-Lab, CLAHE, image enhancement, moon crescent.

1. Introduction

Image enhancement is an essential step in image processing. It improves an image's quality and visual appearance, so that the output is best suited for a specific goal [1]. Image enhancement techniques are used in different applications, such as face [2] and fingerprint recognition [3], watermarking [4], medical image processing [5]–[9] and many others [10], [11]. The aim is to achieve the finest image quality possible, since it influences the accuracy of information retrieval and interpretation process. Because each situation may necessitate a different approach, we should choose an enhancement technique based on the problems at hand and the properties of the image. Therefore, numerous enhancement methods have been proposed.

Medical imaging principles, for example, differ from general imaging principles. According to [8], many factors, such as the system used, random noise, sensor sensitivity, analogue-to-digital conversion and so on, may impact the quality of medical imaging. Blurred edges and low contrast are experienced frequently, necessitating the need to enhance and highlight the image's detailed features in order to diagnose the disease. Some of the medical image enhancement methods have been proposed in recent years by [5]–[8]. Paper [5] proposed a generalized training approach that integrates previous anatomical information into CNNs via a new end-to-end regularization model. The new framework encourages models to adopt the underlying anatomy, referred to as image priors, through learnt nonlinear representations of the shape. Article [6] used an adaptive threshold and an improved fuzzy set based on the nonsubsampled contourlet transform (NSCT). The authors divided the original image into the NSCT domain using a low-frequency sub-band and multiple high-frequency sub-bands before applying a linear transformation to the coefficients of the low frequency component. They utilized an adaptive threshold technique to remove high-frequency image noise, and increased the global contrast level and enhanced image details by using an improved fuzzy set and the Laplace operator.

Enhancement techniques for satellite images are a promising trend, and there are several possibilities for improving the visual quality of remotely sensed images. Paper [12] reviewed several hyperspectral image enhancement methods and categorized them as non-fusion-based and fusion-based. Non-fusion-based enhancement methods concentrate on the spatial resolution of hyperspectral imaging systems. Meanwhile, their fusion-based counterparts combine a low spatial resolution hyperspectral image with auxiliary information to generate a high spatial resolution scene. Examples of non-fusion-based methods include the one proposed by [13]. Its authors trained BPNN relying on the learning-based technique and using low-resolution images and down-sampled versions. Then, they performed a super-resolution by taking into account the spatial correlation of various materials in hyperspectral images. These hyperspec-

tral images were used as training data for enhancing the coherence of the improved and original hyperspectral images. Satellite images are also prone to suffer from uneven illumination. To solve this problem, paper [14] proposed a spatially-adaptive gamma correction (SAGC) method that used relative total variation (RTV). With this method, its authors obtained two types of images with strong and weak structures. The one with strong structures is the base image, and the other one with weak structures, is the detailed image. They used an adaptive gamma correction method to enhance the base image, while an enhancement factor was relied upon to correct the detailed image. Subsequently, by combining these two images, they produced a high-contrast optical remote sensing image. The authors of [15] developed an enhancement method to identify both spatial and spectral response operators using multispectral and hyperspectral fusion models. This method yielded colors and brightness that were more akin to a low-resolution hyperspectral image.

In [16], the authors conducted an in-depth review of more than 120 underwater image enhancement and restoration studies. Remarkable progress that took place in underwater image visual quality in recent years was observed. The authors grouped the underwater enhancement methods into filtering-based methods, color correction-based methods, image fusion-based methods and deep learning-based methods. Article [17] proposed utilizing a turbid image to produce a color-corrected image and a contrast-enhanced image using the fusion technique. These two images were combined using four weight maps: Laplacian contrast, local contrast, saliency, and exposedness. The authors of [18] used a convolutional neural network-based image enhancement model to train a synthetic underwater image database. Their model relied on an automated end-to-end and data-driven training process to reconstruct a clear latent underwater image.

To the best of our knowledge, there is currently a lack of studies on enhancing telescopic images over medical, remote sensing, or underwater images. However, the importance of the analysis of telescope-obtained images is the same as for other types of images. In this paper, we start by analyzing the importance of studying the visibility of the moon crescent in astronomy. There are many methods for determining when the holy months of Ramadan (fasting), Syawal (Hari Raya), and Zulhijjah (pilgrimage) begin. Several countries, such as Malaysia, Brunei, Indonesia, and Singapore, use the Imkanurrukyah (Rukyah and Hisab) technique. The crescent is defined as the moon crescent after the ijtimak that first appears or visibles after sunset. Physically, the current phase of the moon is small in size and is close to the position of the setting sun. In addition, the appearance of the crescent is influenced by several other factors, such as the position of the crescent, sunlight refraction, sky brightness and the rate of atmospheric extinction. Therefore, it is quite difficult to notice it. The appearance of the moon crescent is discussed, from a scientific point of view, in physical terms. Physical knowledge is used to per-

form calculations on the movement of the moon, the earth and the sun and to ensure that the following Imkanurrukyah criteria have been met [19]:

- the moon's altitude at sunset must be at least 2 degrees, and the elongation between the moon and the sun must be at least 3 degrees, or

- the moon's age after conjunction is at least 8 hours when the moon sets.

However, MABIMS agreed to use new criteria: moon's altitude at sunset must be at least 3 degrees and the elongation between the moon and the sun must be at least 6.4 degrees [20].

Various methods have been developed to determine the visibility limit of the youngest moon crescent that can be seen and observed in essence [21]. In the Rukyah method, new tools are used, such as a large telescope attached to a digital camera, for imaging the new moon crescent [22]. The use of large telescopes ensures a high degree of magnification and enhances the ability to identify the moon crescent. But the high amplification rate results also in high noise levels [23]. Moreover, no significant differences exist between the crescent and its background, making it indistinguishable [24]. Therefore, this paper aims at increasing visibility of the moon crescent through a method that is not new, but still relevant, namely by relying on CLAHE and bilateral filtering. We organize the remainder of the paper as follows. Section 2 presents some related works using CLAHE. Section 3 contains a description of the proposed work. The results are discussed in Section 4. Finally, Section 5 concludes the paper.

2. Related Works

Histogram equalization (HE) is a relatively simple image processing method used for adjusting contrast based on the image's histogram. In article [25], a comprehensive study of HE-based contrast enhancement methods was conducted. HE typically improves the global contrast of images with poor lighting. It re-maps the image's grayscale, so that the distribution of the resulting histogram is as close as possible to being uniform. With this adjustment, the intensities on the histogram can be dispersed more evenly. It improves contrast in areas with low local contrast. Although this approach is very straightforward to apply as it is less computationally demanding, it has the disadvantage of increasing the contrast of background noise while diminishing the usable sign. The adaptive histogram equalization (AHE) technique, as opposed to the standard approach, is capable of providing significantly better results in this situation.

AHE, which was independently developed by [26]–[28], differs from conventional HE. The adaptive method computes a histogram for each distinct section of the image. These histograms are used to redistribute the image's lightness values. Consequently, AHE is suitable for enhancing

edge definitions and improving local contrast in each region of the image. AHE has the disadvantage of being computationally slow. In addition, it tends to overamplify noise in the homogenous regions of the image. Consequently, paper [29] proposed a variation of AHE called contrast limited adaptive histogram equalization (CLAHE) in order to increase its speed and improve the enhanced image. Paper [29] showed the great success of their CLAHE algorithm applied to a computer tomography (CT) image of the chest, surface coil MRI of the spine and an X-ray angiogram. CLAHE has been widely applied to improve image contrast in various computer vision and pattern recognition applications [30]–[33].

With the current global pandemic, COVID-19 detection is a crucial challenge for medical practitioners. Medical practitioners have utilized a variety of tools and strategies to detect and prevent COVID-19 transmission. Paper [34] introduced the COVIDLite technique in which the white balance method is followed by CLAHE. Then, an analysis is performed by a depth-wise separable convolutional neural network in order to help radiologists detect COVID-19 patients based on CXR images. The authors of [35] used CLAHE to detect COVID-19 infections using CT lung scans. Additionally, they classified the images using a convolutional neural network (CNN). In [36], a pretty similar approach as that adopted by [35] is used to classify a total of 100 X-Ray chest images of COVID-19 patients as well as 100 X-Ray chest images of healthy individuals. Paper [37] improved the sensitivity of chest X-rays utilizing the pipeline for advanced contrast enhancement (PACE) method. This nonlinear post-processing approach combines adequately fast and adaptive bidimensional empirical mode decomposition (FABEMD) and CLAHE. Based on this highlight, CLAHE is still being adopted and is increasingly important in improving image quality.

3. Proposed Work

To solve the issues discussed in Section 1, we adopt the CLAHE method to increase the visibility of the moon crescent in an image. Our enhancement approach consists of several steps. CLAHE is applied to the L component of the Lab color space to adjust the lightness contrast in the first step. After that, we convert the transformed image back to an RGB image. Then, we perform contrast enhancement
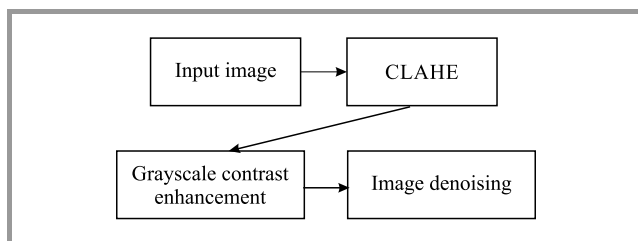
on a selected component of the transformed RGB image. Finally, we utilize the image denoising step, using bilateral filtering, to reduce noise caused by the contrast enhancement process. Figure 1 illustrates the proposed enhancement approach for improving the visibility of the moon crescent.

3.1. CLAHE on Lab Image

Paper [29] proposed CLAHE to overcome contrast over-amplification introduced by AHE. CLAHE clips the histogram using a contrast factor, called a clip limit, that prevents over-saturation of the image, especially in homogeneous areas. A variation of the contrast-limited technique, called adaptive histogram clip (AHC), can also be used to moderate the over-enhancement of background regions of images. It works by adjusting the clipping level. The Rayleigh distribution is one of the AHC that normally used, producing a bell-shaped histogram. The function is defined as follows:

$$Rayleigh_g = g_{\min} + \left[2(\alpha^2) \ln \left(\frac{1}{1 - P_f} \right) \right]^{0.5}. \quad (1)$$

In this function, g_{min} denotes a minimum pixel value. Cumulative probability distribution is written as $P(f)$, and α is a positive real scalar specifying the distribution parameter. The clip limit in this study is set to equal 0.005 and α value in the Rayleigh distribution function is set to 0.04.

The Lab color space mathematically defines all perceptible colors in three dimensions: L for lightness, a and b for the four color components of human visions: red, green, blue and yellow. The name "lab" comes from the Hunter 1948 color space. L*, a*, and b* values are typically absolute and have a predetermined range. L* = 0 yields the darkest black, and L* = 100 indicates the brightest white. In contrast to the RGB and CMYK color models, Lab color is intended to simulate human perception. It strives for perceptual consistency, and its L component closely corresponds to the human experience of lightness. Therefore, we modify the lightness contrast using the L component, as illustrated in Fig. 2.
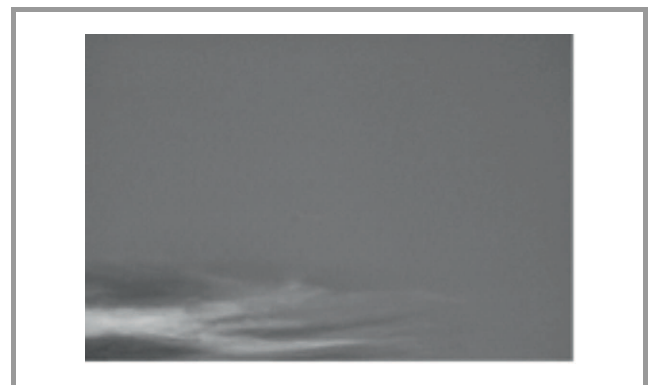

Fig. 1. The approach proposed to enhance the visibility of the moon crescent.
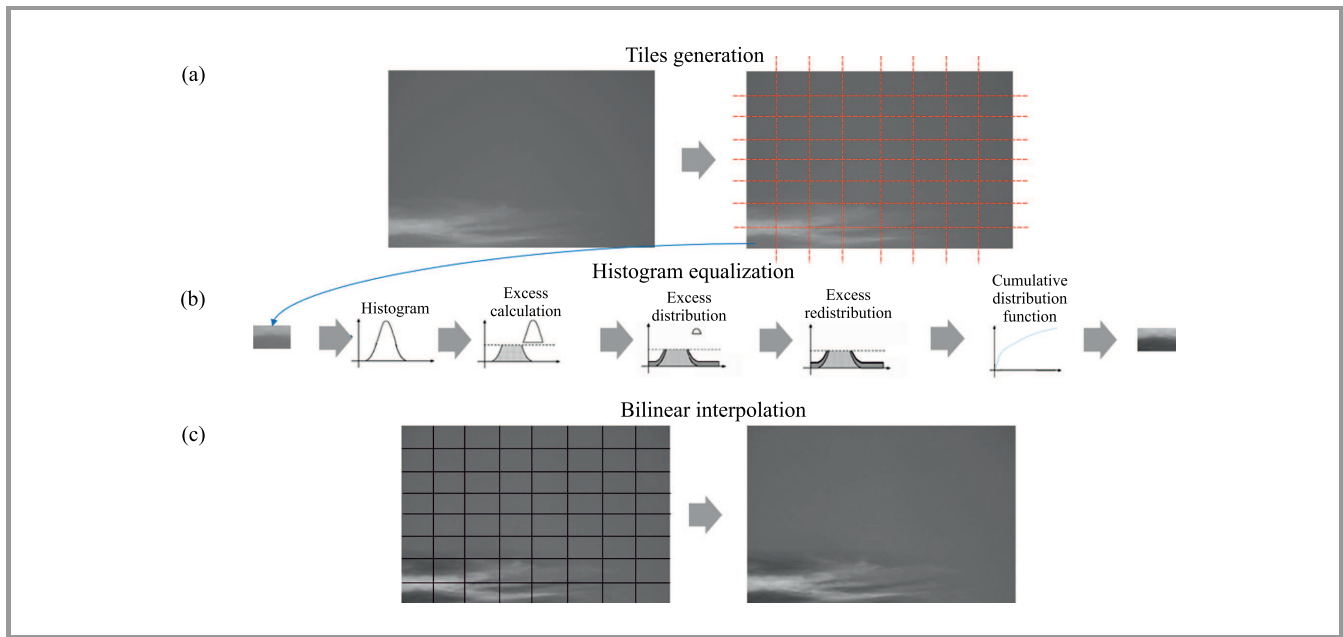

Fig. 2. L component of Lab image.

Fig. 3. CLAHE applied on L component of Lab color space.

The CLAHE algorithm, as presented in Fig. 3, is composed of three major parts:

1. Tile generation. The input image L is scaled into a range of [0–1] by dividing the L component by 100. As shown in Fig. 3a, it is first divided into 8×8 sections called tiles.

2. Histogram equalization. This part consists of five steps:

   - Histogram computation. On each tile, calculate the histogram as a set of bins.
   - Excess calculation. Accumulate the histogram bin values that exceed the clip limit.
   - Excess distribution. Then, distribute them into other bins.
   - Excess redistribution. The redistribution will push specific bins back over the clip limit, allowing for an efficient clip limit that is more considerable than the specified limit, with its exact value depending on the image. If this is undesirable, recursively perform the redistribution procedure until the excess is negligible.
   - Scaling and mapping. Calculate the cumulative distribution function (CDF) for the histogram values. Then, scale and map the CDF values of each tile using the input image pixel values.

3. Bilinear interpolation. The resulting tiles are stitched using bilinear interpolation to improve the image contrast.

To convert again into RGB, we rescale the L component in the range of [0–100] by multiplying it by 100. In short,
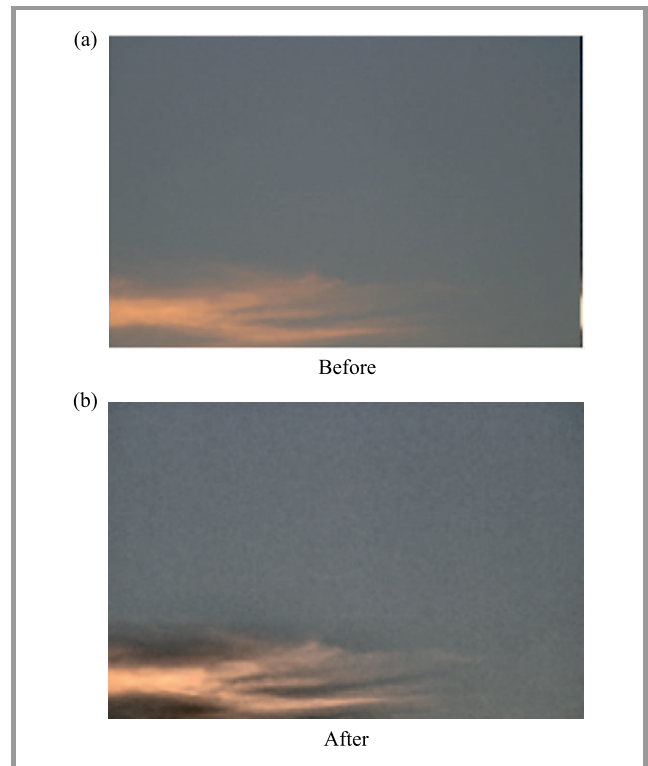

Fig. 4. Result of CLAHE on Lab color space.

given an input image, a desire output image generated from CLAHE on Lab image is shown in Fig. 4. As per Fig. 4b, the image after CLAHE contains more detailed information, especially around the reddish-orange color part of the cloud.

To show that CLAHE is better than its counterpart in enhancing image quality, Fig. 5 presents images and their
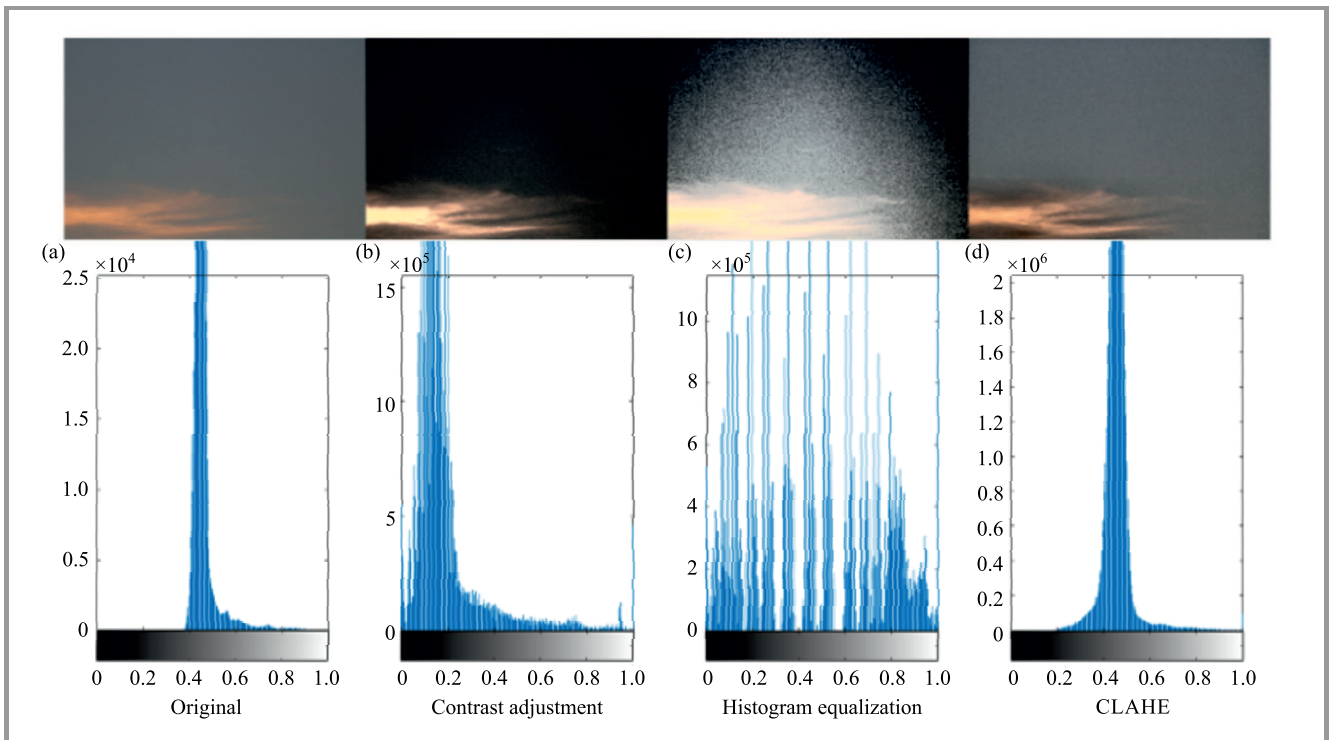
Fig. 5. Comparison between CLAHE and other enhancement techniques.

histogram distributions obtained with the use of three different methods. The left-most image is the original image. The second image is obtained by contrast adjustment (CA), while the third and the last images are obtained by using histogram equalization (HE) and CLAHE, respectively. It may be noticed in Fig. 5 that the original image consists primarily of grey color and a little bit of reddish-orange color, meaning that the middle bins show higher frequencies than the left and the right bins. When the CA process is applied, it saturates the bottom 1% and the top 1% of all pixel values, making the grey colors look darker and the reddish-orange color looks brighter than the original. HE distributes pixels equally at all levels, producing a uniform distribution of grey levels for the resulting image, but eventually, much noise is produced with this technique. Meanwhile, the result of CLAHE shows that it is clearly superior in preserving details and enhances the quality of the image significantly.

3.2. Grayscale Contrast Enhancement

The resulting image obtained from the previous process is used to select a component that is characterized by good moon crescent visibility. To do this, we calculate image histograms for the separated components. For each component, the histograms are distributed into three bins: 0, 0.5 and 1. The selection of components is based on the highest number of the middle bin (0.5 value), as compared to the left (0 value) and right (1 value) bins. This component is considered to be our grayscale image and is denoted by $G(x,y)$.
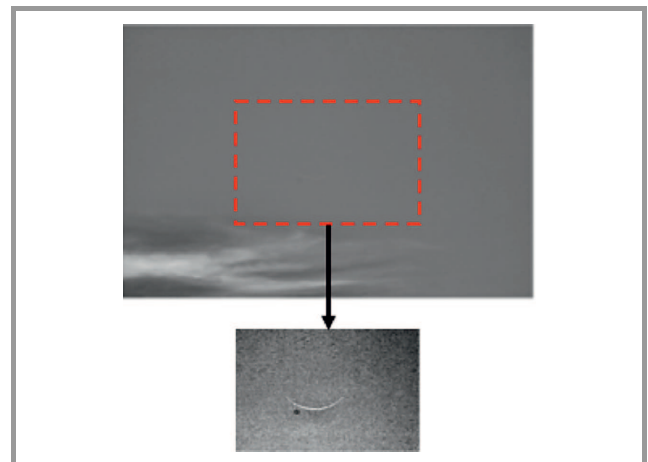

Fig. 6. Example of a result obtained with the grayscale contrast enhancement technique (bottom image). The upper CLAHE image is cropped to create the image at the bottom.

Next, we perform an auto-cropping process on the image to select the region of interest, $I(x,y)$. Based on the available data we know, that the moon is normally located in the center of the image. Therefore, the cropping process is performed by estimating the moon area from the center of the image with 40% of the original size (see Fig. 6). Using this cropped image, we further perform grayscale contrast enhancement by adjusting the image histogram based on the image's standard deviation. It is simply estimated using the following familiar expressions for mean, m and standard deviation, σ:

$$m = \frac{1}{MN} \sum_{x=0}^{M-1} \sum_{y=0}^{N-1} I(x,y) \qquad (2)$$

and

$$\sigma = \sqrt{\frac{1}{MN} \sum_{x=0}^{M-1} \sum_{y=0}^{N-1} \left[I(x,y) - m \right]^2} \; . \qquad (3)$$

For $x = 0, 1, 2 \dots, M-1$ and $y = 0, 1, 2, \dots, N-1$. The histogram is stretched in the range between $[m - 2\sigma, m + 2\sigma]$.

3.3. Bilateral Filtering

The backgrounds of images with high magnification rates are characterized by high noise levels, similar to the well-known salt and pepper noise. We perform a bilateral filtering process to denoise and smooth the region's boundaries, since it is both an edge-preserving and noise reduction non-linear smoothing filter. The name of the bilateral filtering procedure was assigned by [38]. It replaces each pixel's intensity with a weighted average of intensity values from the neighboring pixels. The algorithm starts with an inspection of a patch from the sky portion of the image. Then, we compute the variance of the patch to approximate noise variance.

$$\sigma_p^2 = \frac{1}{ST} \sum_{x=0}^{S-1} \sum_{y=0}^{T-1} \left[P(x,y) - m \right]^2 \; , \qquad (4)$$

with m being calculated using Eq. (2). The bilateral filter, BF is formulated as follows:

$$BF[I]_p = \frac{1}{W_p} \sum_{q \in s} G_{\sigma_s}(p-q) G_{\sigma_r}(I_p - I_q) I_q \; , \qquad (5)$$

where W_p is a normalization factor:

$$W_p = \sum_{q \in s} G_{\sigma_s}(p-q) G_{\sigma_r}(I_p - I_q) \qquad (6)$$

and $G_\sigma(x)$ denotes the two-dimensional Gaussian kernel:

$$G_\sigma(x) = \frac{1}{2\pi\sigma^2} e^{-\frac{x^2}{2\sigma^2}} \; . \qquad (7)$$

Parameters σ_s and σ_r in Eq. (5) will be used to calculate the amount of filtering applied to image I. Equation (6) is a normalized weighted average in which G_{σ_s} is a spatial Gaussian that reduces the effect of distant pixels and G_{σ_r} is a range Gaussian that reduces the influence of pixels q with an intensity value different from I_p. It is worth noting that the term "range" refers to amounts relative to pixel values, as opposed to space, which refers to pixel location. Figure 7 depicts an example of the output of the bilateral filter.
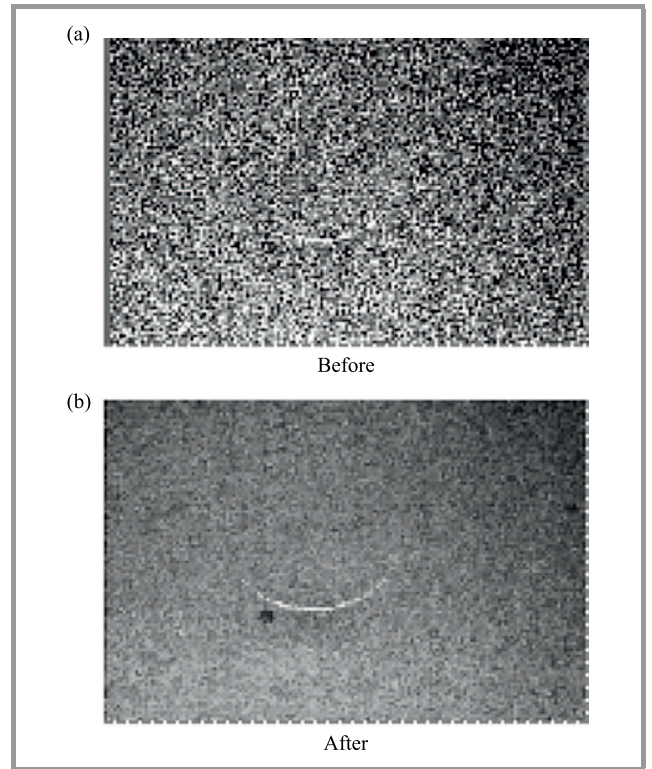

Fig. 7. Result before and after bilateral filtering of the cropped image.

4. Results and Discussion

The enhancement algorithm seeks to increase image quality by generating a processed image that is superior to the original image, for further processing. Such an improvement might be evaluated subjectively through a visual assessment of the image, or objectively through statistical measurements. In this paper, fifteen images are tested and analyzed with the proposed method. The images were obtained from Jabatan Kemajuan Islam Malaysia (JAKIM), Teluk Kemang Observatory and Pejabat Mufti Negeri Terengganu. All images were captured at different times using different types of equipment and were saved in jpeg and png formats. In Fig. 8, we present four examples of telescope-obtained images used in this study. As shown in Fig. 8c and Fig. 8d, the moon is invisible to the naked eye. Noise is present in Fig. 8a and Fig. 8b, hindering further processing.

The results obtained from the experiment are presented in Fig. 9. As demonstrated in the figure, the proposed method performed successfully for all images, proving its usefulness. The combination of CLAHE and grayscale contrast enhancement successfully increases the visibility of the moon crescent, even when it is invisible to the naked eye. Bilateral filtering (BF) was performed by smoothing the region concerned. The results were obtained with the bilateral filter using the same variance, σ_r of the range Gaussian kernel, which is set to double the variance of noise, σ_p^2 obtained from Eq. (3). However, we set σ_s to different values. The leftmost images are the results of CLAHE

(a)

Syaban 1432H, time taken: 2 July 2011 at 7:45 PM

(b)

Rabiulawal 1439H, time taken: 19 Nov. 2017 at 6:56 PM

(c)

Rejab 1437H, time taken: 8 April 2016 at 7:23 PM

(d)

Syaban 1438H, time taken: 27 April 2017 at 7:36 PM

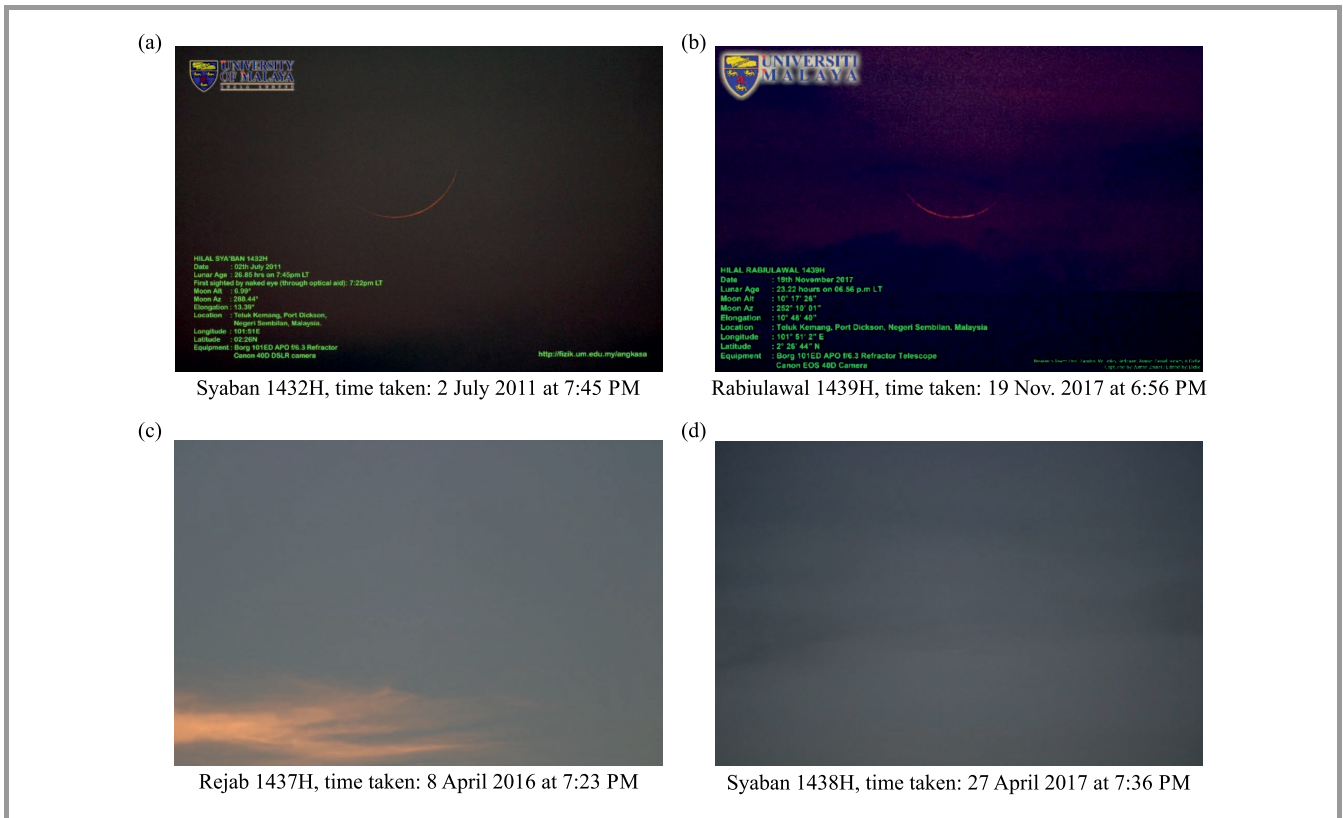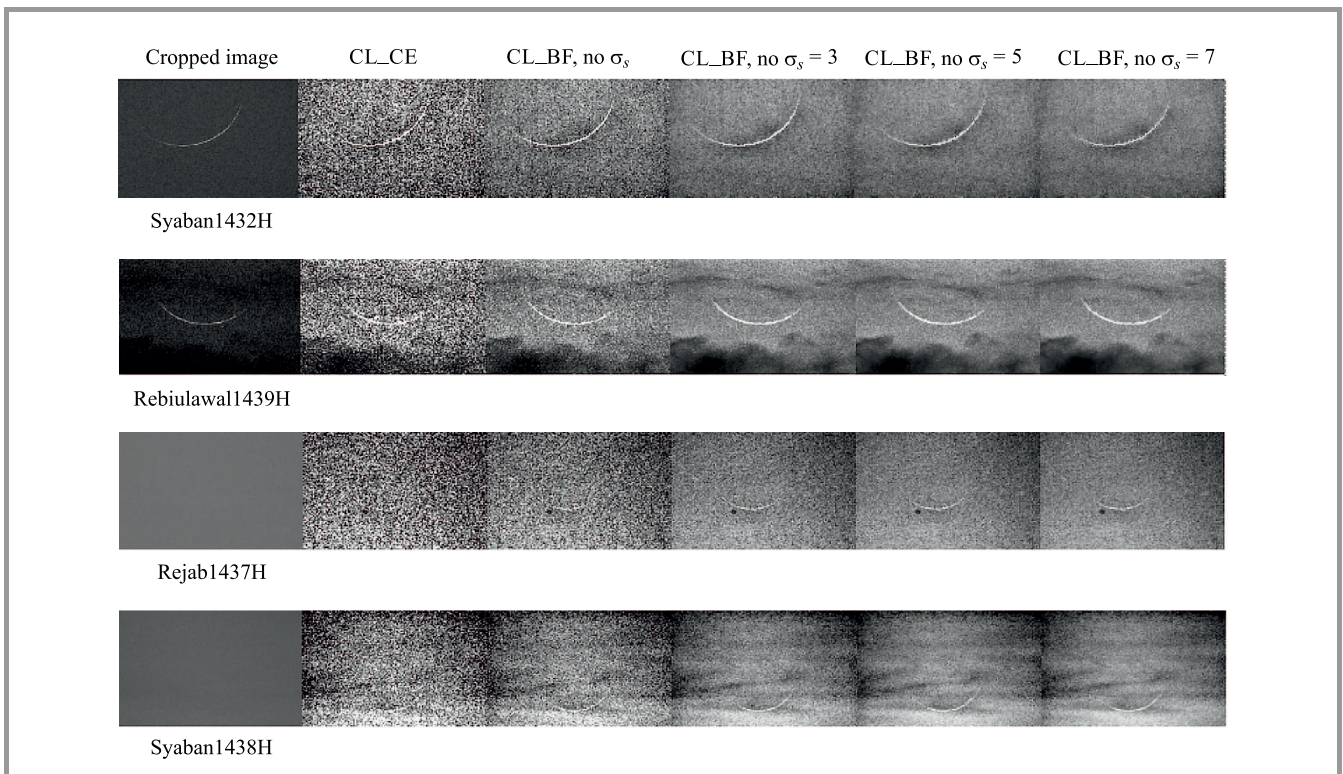*Fig. 8.* Telescope-obtained images.

Fig. 9. Results obtained with the contrast enhancement and bilateral filtering methods, using different σ_s on the cropped CLAHE images.

Table 1

Comparison of PSNR and MSE values between contrast enhancement and bilateral filtering (BF) of different σ_s

Image	CL_CE	CL_BF				CL_CE	CL_BF			
		–	3	5	7		–	3	5	7
1	58.12	59.66	60.21	60.28	60.31	0.05	0.03	0.02	0.01	0.01
2	57.17	58.23	58.45	58.47	58.47	0.12	0.10	0.09	0.09	0.09
3	60.70	63.51	66.27	67.00	67.28	0.05	0.03	0.02	0.01	0.01
4	60.07	61.42	62.30	62.45	62.50	0.06	0.05	0.04	0.04	0.04
5	61.78	64.67	65.83	66.24	66.56	0.04	0.02	0.02	0.02	0.01
6	59.27	59.40	59.44	59.45	59.46	0.08	0.07	0.07	0.07	0.07
7	64.57	69.43	70.44	70.49	70.51	0.02	0.01	0.01	0.01	0.01
8	59.61	59.71	59.79	59.83	59.86	0.10	0.07	0.06	0.06	0.06
9	60.39	61.65	62.01	62.08	62.13	0.06	0.04	0.04	0.04	0.04
10	63.51	63.76	63.96	64.14	64.30	0.03	0.03	0.03	0.03	0.02
11	59.73	61.30	61.93	62.00	62.03	0.07	0.05	0.04	0.04	0.04
12	63.45	63.98	64.10	64.13	64.14	0.03	0.03	0.03	0.03	0.03
13	60.43	62.69	64.67	65.11	65.28	0.06	0.04	0.02	0.02	0.02
14	60.42	60.80	61.05	61.09	61.10	0.06	0.06	0.05	0.05	0.05
15	63.41	66.26	66.48	66.43	66.43	0.03	0.02	0.01	0.01	0.01

grayscale contrast enhancement (CL_CE). Images presented in column two are the results of CLAHE bilateral filtering (CL_BF) without σ_s, while those in columns three to five are the results of CLAHE bilateral filtering with $\sigma_s = 3$, $\sigma_s = 5$, and $\sigma_s = 7$, respectively. As can be observed from the figure, as σ_s increases, the images become smoother. However, the moon crescent becomes a little bit blurry. This can be seen based on the example of images zoomed around the moon crescent of bilateral filter with $\sigma_s = 3$ and $\sigma_s = 7$, as presented in Fig. 9.

Based on Table 1, CL_BF shows better PSNR values than CL_CE for all images. With CL_BF, increasing the σ_s improve the quality of enhanced image where PSNR for all images with $\sigma_s = 7$ is higher than the PSNR with the lower setting. However, for all enhanced images, the difference of CL_BF between $\sigma_s = 7$ and $\sigma_s = 3$ is less than 1.0 except for image 3. Similar to the MSE, for all enhanced images, changing the size of σ_s do not show much difference. Note that increasing the σ_s is actually increase the neighborhood size, which increases the filter execution time. So, using a small size of σ_s is enough in this case.

5. Conclusion

This paper described how to improve moon crescent images with the use of CLAHE, grayscale contrast enhancement, and bilateral filtering methods. We began by converting an RGB image into CIELab color space. CLAHE was applied to the L component of the image in order to improve visibility, before converting it back to an RGB image. The gray image was then chosen based on the R, G, or B component with the highest gray bin value (bin value = 0.5). After

that, we cropped the image to focus on the moon crescent, before enhancing the contrast of the grayscale image. This process was performed by adjusting the image's histogram based on the standard deviation of the image. In the last step, the bilateral filtering process was performed to remove noise resulting from grayscale contrast enhancement. The experiment conducted on fifteen moon crescent images demonstrates that our method has acceptable practical results. The moon crescent that is invisible in the original images may be seen after enhancing them with the use of the proposed method.

Acknowledgements

References

[1] J. R. Tang and N. A. M. Isa, "Bi-histogram equalization using modified histogram bins", *Applied Soft Comput.*, vol. 55, 2017, pp. 31–43 (DOI: 10.1016/j.asoc.2017.01.053).

[2] M. O. Oloyede, G. P. Hancke, and H. C. Myburgh, "Improving face recognition systems using a new image enhancement technique, hybrid features and the convolutional neural network", 2018, *IEEE Access*, vol. 6, pp. 75181–75191 (DOI: 10.1109/ACCESS.2018.2883748).

[3] R. Gupta, M. Khari, D. Gupta, and R. G. Crespo, "Fingerprint image enhancement and reconstruction using the orientation and phase reconstruction", *Information Sci.*, 2020, vol. 530, pp. 201–218 (DOI: 10.1016/j.ins.2020.01.031).

[4] O. Juarez-Sandoval *et al.*, "Improved unseen-visible watermarking for copyright protection of digital image", in *Proc. IEEE 5th Int. Workshop on Biometrics and Forensics (IWBF)*, Coverty, UK, 2017, pp. 1–5 (DOI: 10.1109/IWBF.2017.7935084).

[5] O. Oktay *et al.*, "Anatomically constrained neural networks (AC-NNs): application to cardiac image enhancement and segmentation", *IEEE Trans. on Medical Imaging*, 2018, vol. 37, no. 2, pp. 384–395 (DOI: 10.1109/TMI.2017.2743464).

[6] F. Zhou, Z. Jia, J. Yang, and N. Kasabov, "Method of improved fuzzy contrast combined adaptive threshold in NSCT for medical image enhancement", *BioMed Res. Int.*, vol. 2017, 10 pages, 2017 (DOI: 10.1155/2017/3969152).

[7] J. Li, X. Zeng, and J. Su, "Medical image enhancement algorithm based on biorthogonal wavelet", *Acta Microscopica*, vol. 28, no. 1, 2019, pp. 100-107.

[8] T. Qiu *et al.*, "Efficient medical image enhancement based on CNN-FBB model", *IET Image Processing*, vol. 13, no. 10, pp. 1736–1744, 2019 (DOI: 10.1049/iet-ipr.2018.6380).

[9] K. J. Xia, J. Q. Wang, and J. Cai, "A novel medical image enhancement algorithm based on improvement correction strategy in wavelet transform domain" *Cluster Comput.*, vol. 22, no. 5, pp. 10969–10977, 2019 (DOI: 10.1007/s10586-017-1264-y).

[10] J. S. Chiang *et al.*, "Adaptive image enhancement method for document", in *Proc. IEEE Int. Symp. on Intelligent Signal Process. and Commun. Systems (ISPACS)*, Xiamen, China, 2017, pp. 417–420 (DOI: 10.1109/ISPACS.2017.8266515).

[11] M. Gharbi, J. Chen, J. T. Barron, S. W. Hasinoff, and F. Durand, "Deep bilateral learning for real-time image enhancement", *ACM Trans. on Graphics (TOG)*, vol. 36, no. 4, pp. 1–12 (DOI: 10.1145/3072959.3073592).

[12] R. Ablin, C. H. Sulochana, and G. Prabin, "An investigation in satellite images based on image enhancement techniques", *European J. of Remote Sens.*, vol. 53, no. Sup. 2, pp. 86–94 (DOI: 10.1080/22797254.2019.1673216).

[13] X. Han, J. Yu, J. Luo, and W. Sun, "Hyperspectral andmultispectral image fusion using cluster-based multi-branch BP neural networks", *Remote Sens.*, vol. 11, no, 10, 2019 (DOI: 10.3390/rs11101173).

[14] Z. Huang *et al.*, "Optical remote sensing image enhancement with weak structure preservation via spatially adaptive gamma correction", *Infrared Physics & Technol.*, vol. 94, pp. 38–47, 2018 (DOI: 10.1016/j.infrared.2018.08.019).

[15] Q. Xie *et al.*, "Multispectral and hyperspectral image fusion by MS/HS fusion net", in *Proc. of the IEEE Conf. on Computer Vision and Pattern Recognition*, Long Beach, CA, USA, 2019, pp. 1585–1594 (DOI: 10.1109/CVPR.2019.00168).

[16] M. Yang, J. Hu, C. Li, G. Rohde, Y. Du, and K. Hu, "An in-depth survey of underwater image enhancement and restoration", *IEEE Access*, vol. 7, pp. 123638–123657, 2019 (DOI: 10.1109/ACCESS.2019.2932611).

[17] C. O. Ancuti, C. Ancuti, C. De Vleeschouwer, and P. Bekaert, "Color balance and fusion for underwater image enhancement, *IEEE Trans. on Image Process.*, vol. 27, no. 1, pp. 379–393, 2018 (DOI: 10.1109/TIP.2017.2759252).

[18] S. Anwar, C. Li, and F. Porikli, "Deep underwater image enhancement", *ArXiv*, 2018 [Online]. Available: https://arxiv.org/pdf/1807.03528.pdf

[19] M. Azhari, "Penetapan Awal bulan Hijriah: Ramadan, Syawal dan Zulhijjah 1433 H/ 2012 M", *NRE Executive Discourse*, pp. 1–22, 2012 (in Malaysian).

[20] T. Djamaluddin, "Menuju Kriteria Baru MABIMS Berbasis Astronomi", 2016 [Online]. Available: https://tdjamaluddin.wordpress.com/2016/10/05/menuju-kriteria-baru-mabims-berbasis-astronomi/ (in Indonesian)

[21] K. Wahid, M. S. A. M. Nawawi, S. Man, and N. Ahmad, "Teknik Cerapan Anak Bulan: Satu Penelitian Literatur (Observation Techniques of Crescent: A Literature Review)", *UMRAN-Int. J. of Islamic and Civilizational Studies*, vol. 6, no. 3, pp. 47–55, 2019 (DOI 10.11113/umran2019.6n3.349). (in Malaysian)

[22] A. Joko Satria, C. W. Loon, and N. Ahmad, "Pensabitan Hilal Menerusi Teknik Pengimejan. Dalam Dimensi Penyelidikan Astronomi Islam", Saadan Man *et al.* Eds., Kuala Lumpur: Jabatan Fiqh dan Usul, Akademi Pengajian Islam, Universiti Malaya, 2013, vol. 95 (in Malaysian).

[23] M. Fakhar, P. Moalem, and M. A. Badri, "Lunar crescent detection based on image processing algorithms", *Earth, Moon, and Planets*, vol. 114, no. 1, pp. 17–34, 2014 (DOI: 10.1007/s11038-014-9449-3).

[24] M. N. M. Yatim, A. Haron, and A. Mohamed, "New Moon Observation Online Records", *2nd Int. Conf. on Islamic App. in Computer Sci. and Technol. (IMAN2014)*, Amman, Jordan, Paper ID: 72, 2014.

[25] M. Kaur, J. Kaur, and J. Kaur, "Survey of contrast enhancement techniques based on histogram equalization", *Int. J. of Adv. Computer Sci. and App.*, vol. 2, no. 7, 2011 (DOI: 10.14569/IJACSA.2011.020721).

[26] D. J. Ketcham, "Real-time image enhancement techniques", in *Image Processing*, vol. 74, pp. 120–125, 1976 (DOI: 10.1117/12.954708).

[27] R. Hummel, "Image enhancement by histogram transformation", *Computer Graphics Image Process.*, vol. 6, no. 2, pp. 184–195, 1977 (DOI: 10.1016/S0146-664X(77)80011-7).

[28] S. M. Pizer, "Intensity mappings for the display of medical images", *Functional Mapping of Organ Systems and Other Computer Topics*, Society of Nuclear Medicine, pp. 205–217, 1981.

[29] S. M. Pizer *et al.*, "Adaptive histogram equalization and its variations", *Computer Vision, Graphics, and Image Process.*, vol. 39, no. 3, pp. 355–368, 1987 (DOI: 10.1016/S0734-189X(87)80186-X).

[30] T. Ayyavoo and J. J. Suseela, "Illumination pre-processing method for face recognition using 2D DWT and CLAHE", *IET Biometrics*, vol. 7, no. 4, pp. 380–390, 2017 (DOI:10.1049/iet-bmt.2016.0092).

[31] L. Li, Y. Si, and Z. Jia, "Medical image enhancement based on CLAHE and unsharp masking in NSCT domain", *J. of Medical Imaging and Health Informatics*, vol. 8, no. 3, pp. 431–438, 2018 (DOI: 10.1166/jmihi.2018.2328).

[32] J. Ma, X. Fan, S. X. Yang, X. Zhang, and X. Zhu, "Contrast limited adaptive histogram equalization-based fusion in YIQ and HSI colour spaces for underwater image enhancement", *Int. J. of Pattern Recognition and Artificial Intell.*, vol. 32, no. 7, 2018 (DOI: 10.20944/preprints201703.0086.v1).

[33] S. Sahu, A. K. Singh, S. P. Ghrera, and M. Elhoseny, "An approach for de-noising and contrast enhancement of retinal fundus image using CLAHE", *Optics & Laser Technol.*, vol. 110, pp. 87-98, 2019 (DOI: 10.1016/j.optlastec.2018.06.061).

[34] M. Siddhartha and A. Santra, "COVIDLite: A depth-wise separable deep neural network with white balance and CLAHE for detection of COVID-19", *ArXiv*, 2020 [Online]. Available: https://arxiv.org/pdf/2006.13873.pdf

[35] R. M. James and A. Sunyoto, "Detection Of CT-Scan Lungs COVID-19 Image Using Convolutional Neural Network And CLAHE", in *Proc. IEEE 3rd Int. Conf. on Informat. and Commun. Technol. (ICOIACT)*, Yogyakarta, Indonesia, 2020, pp. 302–307 (DOI: 10.1109/ICOIACT50329.2020.9332069).

[36] B. K. Umri, M. W. Akhyari, and K. Kusrini, "Detection of Covid-19 in Chest X-ray Image using CLAHE and Convolutional Neural Network, in *2nd IEEE Int. Conf. on Cybernet. and Intelligent System (ICORIS)*, Manado, Indonesia, 2020, pp. 1–5 (DOI: 10.1109/ICORIS50180.2020.9320806).

[37] G. Siracusano *et al.*, "Pipeline for Advanced Contrast Enhancement (PACE) of Chest X-ray in Evaluating COVID-19 Patients by Combining Bidimensional Empirical Mode Decomposition and Contrast Limited Adaptive Histogram Equalization (CLAHE)", *Sustainability*, vol. 12, no. 20, 2020 (DOI: 10.3390/su12208573).

[38] C. Tomasi and R. Manduchi, "Bilateral filtering for gray and color images", in *Sixth Int. Conf. on Computer Vision (IEEE Cat. No. 98CH36271)*, Bombay, India, 1998, pp. 839–846 (DOI: 10.1109/ICCV.1998.710815).

Wan Nural Jawahir Hj Wan Yussof is a Senior Lecturer at the Faculty of Ocean Engineering Technology and Informatics at the Universiti Malaysia Terengganu where she has been a faculty member since 2006 as a tutor. Wan Nural Jawahir completed her Ph.D. in 2014. Her research interests lie in the area of computer vision, ranging from theory to design and implementation.

https://orcid.org/0000-0002-3618-1638

E-mail: wannurwy@umt.edu.my

Intelligent Informatics
Faculty of Ocean Engineering Technology and Informatics
Universiti Malaysia Terengganu
21030 Kuala Nerus
Terengganu, Malaysia

Mustafa Man is an Associate Professor at the Faculty of Ocean Engineering Technology and Informatics and also a Deputy Director at the Centre of Research and Innovation Management (CRIM), UMT. He started his Ph.D. in July 2009 and finished his studies in Computer Science at UTM in 2012. He received a Computer Science Diploma, a Computer Science Degree and a Master's Degree from UPM. His research focuses on the development of models for integration of multiple database types, as well as on augmented reality, Android based, and IT related into across domain platform.

https://orcid.org/0000-0003-4071-721X

E-mail: mus@umt.edu.my

Intelligent Informatics
Faculty of Ocean Engineering Technology and Informatics
Universiti Malaysia Terengganu
21030 Kuala Nerus
Terengganu, Malaysia

Roslan Umar pursues his Ph.D. degree from Universiti Malaya (UM), Malaysia in the field of Radio Astronomy. His interest in exploring the universe began during his bachelor degree internship program, when he was assigned to work at the Malaysia National Planetarium. After he finished his M.Sc., Roslan began his academic career at Universiti Sultan Zainal Abidin (UNISZA) and was appointed the Head of Astronomy Unit at UNISZA Observatory. He is currently works as a Senior Lecturer and a research fellow at East Coast Environmental Research Institute (ESERI), UNISZA. Dr. Roslan's research interests are in the field of electromagnetic waves, radio frequency interference, radio astronomy and environmental studies.

https://orcid.org/0000-0002-8413-385X

E-mail: roslan@unisza.edu.my

East Coast Environmental Research Institute (ESERI)
Universiti Sultan Zainal Abidin
21300 Kuala Terengganu
Terengganu, Malaysia

Ahmad Najmuddin Zulkeflee is a Master program student at the East Coast Environmental Research Institute (ESERI), Universiti Sultan Zainal Abidin (UniSZA), where he studies under the supervision of Dr. Roslan Umar. His academic career began by obtaining a Bachelor's degree from Shariah (Islamic) Astronomy Department, Academy of Islamic Studies, University of Malaya (UM).

E-mail: muddinjr97@yahoo.com

East Coast Environmental Research Institute (ESERI)
Universiti Sultan Zainal Abidin
21300 Kuala Terengganu
Terengganu, Malaysia

Ezmahamrul Afreen Awalludin is currently a Senior Lecturer at the Faculty of Fisheries and Food Science, Universiti Malaysia Terengganu. He received his Ph.D. in Computer Science from Universiti Malaysia Terengganu in 2016. His research interests focus on computer vision, image processing and artificial intelligence. He cooperates closely with researchers from a number of different fields, including marine sciences, fisheries and aquaculture, focusing on challenges related to image processing and image-based analysis.

https://orcid.org/0000-0003-4470-0052

E-mail: e.afreen@umt.edu.my

Faculty of Fisheries and Food Science
Universiti Malaysia Terengganu
21030 Kuala Nerus
Terengganu, Malaysia

Nazhatulshima Ahmad has been a senior lecturer at the Department of Physics, Faculty of Science, University of Malaya, since 2013. She has been working at the University since 1999, as a tutor in the Physics Department. She obtained her B.Sc. in Physics from University of Malaya in 1998, M.Sc. (Astronomy) in 2003 and Ph.D. from the same university in 2013. Her main research interests are in emission line stars, such as Be stars, and in binary star systems. She is currently conducting a research project on digital imaging and image processing techniques used for early detection of the young crescent moon.

https://orcid.org/0000-0002-0464-1652

E-mail: n_ahmad@um.edu.my

Department of Physics, Faculty of Science

University of Malaya

50603 Kuala Lumpur

Federal Territory, Malaysia